The effect of interactive ozone chemistry on weak and strong stratospheric polar vortex events

Jessica Oehrlein[1], Gabriel Chiodo[1,2], and Lorenzo M. Polvani[1]

[1]Department of Applied Physics & Applied Mathematics, Columbia University, New York, United States
[2]Department of Environmental Systems Science, Institute for Atmospheric and Climate Science, ETH Zurich, Switzerland

Correspondence: Jessica Oehrlein (jessica.oehrlein@columbia.edu)

Abstract. Modeling and observational studies have reported effects of stratospheric ozone extremes on Northern Hemisphere spring climate. Recent work has further suggested that the coupling of ozone chemistry and dynamics amplifies the surface response to midwinter sudden stratospheric warmings (SSWs). Here, we study the importance of interactive ozone chemistry in representing the stratospheric polar vortex and Northern Hemisphere winter surface climate variability. We contrast two

5 simulations from the interactive and specified chemistry (and thus ozone) versions of the Whole Atmosphere Community Climate Model, designed to isolate the impact of interactive ozone on polar vortex variability. In particular, we analyze the response with and without interactive chemistry to midwinter SSWs, March SSWs, and strong polar vortex events (SPVs). With interactive chemistry, the stratospheric polar vortex is stronger, and more SPVs occur, but we find little effect on the frequency of midwinter SSWs. At the surface, interactive chemistry results in a pattern resembling a more negative North

10 Atlantic Oscillation following midwinter SSWs, but with little impact on the surface signatures of late winter SSWs and SPVs. These results suggest that including interactive ozone chemistry is important for representing North Atlantic and European winter climate variability.

1 Introduction

The climate impacts of stratospheric ozone extremes, particularly Antarctic ozone depletion, have been widely studied (Previdi

15 and Polvani (2014) and references therein). While the effects are clearer and larger in the Southern Hemisphere due to greater ozone depletion, ozone extremes have also been shown to induce springtime surface anomalies in the Northern Hemisphere (Calvo et al., 2015; Ivy et al., 2017).

The weaker ozone depletion in the Northern Hemisphere is partially due to greater interannual variability, which is a result of the larger amplitudes of upward-propagating planetary waves, which perturb the stratospheric circulation. Years with low

20 wave activity tend to a correspond to a stronger vortex and a weaker Brewer-Dobson Circulation (BDC), resulting in weaker ozone transport from the tropics into the poles as well as enhanced formation of polar stratospheric clouds, which contribute to increased springtime destruction of ozone. Years with high wave activity correspond to a weaker vortex and a stronger BDC, with stronger ozone transport from the tropics and temperatures too high for polar stratospheric clouds to form.

These processes are well-represented in fully interactive chemistry-climate models (Strahan and Douglass, 2004). However,

25   such models are computationally expensive compared to the more common ones, in which stratospheric ozone is simply prescribed. A number of studies have explored the importance of interactive ozone chemistry on model representations of coupled stratosphere-troposphere variability. Smith and Polvani (2014) and Karpechko et al. (2014) found little impact of stratospheric ozone extremes on surface climate in the Northern Hemisphere using prescribed zonal mean monthly mean ozone fields. However, Calvo et al. (2015) found robust surface impacts associated with stratospheric ozone extremes using an

30   interactive chemistry-climate model, suggesting the potential importance of this coupling. Further model studies are needed to disentangle the effects of ozone from those of polar vortex variability.

While the effect of polar stratospheric clouds on ozone is mainly seen in the spring when sunlight returns to the region, the variability of the polar vortex can result in wintertime ozone anomalies which may have surface impacts. The most extreme states of the polar vortex are sudden stratospheric warmings (SSWs) and strong polar vortex events (SPVs). Leading up to

35   an SSW, dynamical forcing disrupts the stratospheric circulation, eventually resulting in a reversal of zonal mean zonal wind throughout much of the stratosphere. SSWs have surface effects for the two months following, particularly a negative North Atlantic Oscillation and cold anomalies over much of Northern Eurasia. SPVs, as the result of a lack of planetary wave activity, are not dynamical events in the same way as SSWs (Limpasuvan et al., 2004, 2005) but may still have surface impact (a positive NAO) (Baldwin and Dunkerton, 2001).

40   For the dynamical reasons described above, SSWs and SPVs tend to be associated with the occurrence of positive and negative stratospheric ozone anomalies, respectively. About two weeks prior to an SSW, the BDC accelerates, resulting in adiabatic warming of the stratosphere and enhanced isentropic eddy transport of ozone and thus increased ozone concentration over the pole (De La Cámara et al., 2018). SPVs are similarly accompanied by an anomalously weak BDC because of the lack of planetary wave activity and thus an anomalously low transport of ozone, as well.

45   Because they affect both stratospheric ozone and the NAO in the troposphere, extreme vortex events offer an ideal case in which to study wintertime surface impacts of ozone chemistry. Haase and Matthes (2019) studied the impact of interactive versus prescribed ozone on SSWs, as well as their their surface effects, in simulations of the recent past (1955-present) in an earth system model. They compared results of a simulation with interactive ozone to those of a simulation with ozone prescribed. This prescribed ozone was given daily (with no averaging/climatology) from the historical interactive chemistry

50   simulation. They found a stronger climatological vortex in the interactive chemistry simulation, and this was associated with a decreased SSW frequency. Further, SSWs were followed by stronger and more persistent surface anomalies in the simulation with interactive chemistry. These results suggest important surface impacts of ozone chemistry. However, their simulation was relatively short (64 winters), and the historical period they simulated includes long-term trends in ozone that may affect the results. Also, their method of prescribing ozone means that the ozone in the specified chemistry simulation was associated

55   with dynamical variability of the interactive chemistry run, and that variability was inconsistent with the dynamical state of the specified chemistry model.

Building on the study of Haase and Matthes (2019), we here study interactions between ozone chemistry and polar vortex variability by analyzing SSWs, SPVs, and their surface impacts in two 200-year timeslice simulations with fully interactive

and prescribed chemistry versions of a model. Using 200-year timeslices provides us with a large sample size of SSW and

60 SPV events without long-term ozone trends, and we prescribe ozone based on the ozone climatology from the 200 years of the interactive chemistry simulation. This set of simulations more clearly separates the impact of ozone on the stratosphere-troposphere coupling, via its interannual variation. While we do not see decreased SSW frequency with interactive chemistry, we confirm Haase and Matthes (2019)'s results on the vortex climatology and response to midwinter SSWs. We further find that there is little surface effect of interactive ozone chemistry immediately following SPVs or March SSWs. However, SPVs

65 show long-lasting effects on stratospheric ozone, with anomalies 1-2 months after the central date of a similar magnitude to those caused by midwinter SSWs.

The paper is organized as follows. Section 2 describes the model, simulations, and methodologies. Section 3 addresses our results on the impacts of interactive chemistry, considering the stratospheric mean state, midwinter SSWs, March SSWs, and SPVs. We conclude the paper with a discussion of these results.

70 2   Methods

In this study, we analyze model integrations performed with the Whole Atmosphere Community Climate Model, Version 4 (WACCM4), one atmospheric component of the Community Earth System Model (CESM1) (Marsh et al., 2013). WACCM4 is an interactive chemistry-climate model with a horizontal resolution of 1.9° in latitude and 2.6° in longitude, 66 vertical levels, and a model top at 5.1 $\times 10^{-6}$ hPa (140 km). Northern Hemisphere stratospheric variability, such as the frequency and

75 dynamical features of SSWs, are accurately simulated in WACCM4 (Marsh et al., 2013).

We perform two model integrations, both 200-year-long timeslice integrations with forcings at constant year-2000 values to avoid long-term trends in ozone. One model integration uses the fully interactive chemistry scheme in WACCM4 (Kinnison et al., 2007). We refer to this simulation as the CHEM simulation in the analysis. The other uses the "Specified Chemistry" version of WACCM, known as SC-WACCM (Smith et al., 2014). In the SC-WACCM simulation, ozone concentrations (and

80 a few other radiatively active atmospheric constituents, e.g. CH_4) are prescribed using zonally symmetric, monthly mean, seasonal climatology computed from the WACCM integration. These zonally symmetric monthly ozone fields are read into SC-WACCM and interpolated linearly to the day of the year. More details can be found in Smith et al. (2014). Using the climatology to specify ozone minimizes the effect of ozone extremes in particular years of the interactive chemistry simulation on results of the simulation with prescribed chemistry. We refer to this prescribed chemistry simulation as the NOCHEM

85 simulation in the analysis.

We identify SSWs in the model output following the definition in Charlton and Polvani (2007a) (see the corrigendum Charlton-Perez and Polvani (2011)). We define an SSW as a reversal of zonal mean zonal wind at 60° N and 10 hPa from westerly to easterly during November through March, with the central date being the first day of easterly zonal mean zonal winds. No later date can be a central date until the winds have been westerly again for at least 20 days, and the winds must return

90 to westerly for at least 10 consecutive days before April 30 (thus discarding stratospheric final warmings). This definition is optimal for identifying SSWs, as described by Butler and Gerber (2018). We focus on SSWs occurring in December-February

Atmospheric
Chemistry
and Physics
Discussions

and in March. We consider March events separately from December-February events due both to different shortwave heating behavior and to model bias in March SSW frequency.

To the best of our knowledge, there is no standard definition of an SPV. Different methods have been used in the literature
95 (Limpasuvan et al., 2004; Tripathi et al., 2015; Scaife et al., 2016; Beerli and Grams, 2019). We here follow the definition used in Scaife et al. (2016) and Smith et al. (2018), designed to be analogous to the Charlton and Polvani (2007a) SSW definition and to result in a similar number of events in reanalysis. We define an SPV as zonal mean zonal wind at 60° N and 10 hPa reaching 48 m/s or higher (westerly) during November through March, with the central date being the first day of zonal mean zonal winds above 48 m/s. No later date can be a central date until the winds return below 48 m/s for at least 20 consecutive
100 days. We focus on SPVs occurring in December-February, due to low event frequency in November and March.

The results we present here are based on composites of daily model output for climate variables, with composites centered around SSW or SPV central dates.

For composites from either CHEM or NOCHEM simulations, we calculate significance using a Monte Carlo test based on 5000 randomly chosen central dates. We also consider the difference in CHEM or NOCHEM composites, denoted CHEM-
105 NOCHEM; for these, we calculate significance from a two-sided two-sample t-test.

3   Impact of interactive chemistry

3.1   Stratospheric mean state and extreme events

We first consider the effect of interactive chemistry on the mean state of the stratosphere by examining the climatological Northern Hemisphere 10 hPa zonal mean zonal wind (Figure 1). We find stronger westerlies in CHEM than in NOCHEM in
110 the vortex formation stage (September and early October) and in the latter half of winter (January-April), between $60° - 80°$ N. This relative strength in CHEM in late winter also corresponds to a delayed final warming by 7 days on average (not shown). These results are consistent with those found by Haase and Matthes (2019). The same is not the case in Smith et al. (2014), where the vortex under constant year 1850-conditions was found to be of similar strength with interactive and specified chemistry. The difference in strength of the vortex with interactive vs. specified chemistry is then partially related to forcings
115 used (year 2000 in this study, and 1955-present historical in Haase and Matthes (2019)).

Because we identify extreme stratospheric events using zonal mean zonal winds at 10 hPa and $60° N$ (U1060) (Charlton and Polvani, 2007a; Butler and Gerber, 2018), we next examine the mean state and variability of this quantity in CHEM and NOCHEM. Figure 2 shows the two distributions of U1060 in December through March. The average difference in DJFM between CHEM and NOCHEM is about 1.7 m/s, a small but statistically significant difference; Figure 1 indicates that this
120 difference is larger in January through March. The CHEM distribution also has a longer right tail. This is consistent with the polar vortex being stronger overall with interactive chemistry. It also indicates that we should expect more SPVs in CHEM than in NOCHEM. While there are fewer days of weak westerlies (0-20 m/s) in CHEM than in NOCHEM, the numbers of days of easterlies are similar, so we expect less of a difference in SSW frequency between the two simulations.

Indeed, this is what we find when we calculate the frequencies of weak and strong vortex events in the CHEM and NOCHEM
125 simulations (Table 1). We consider December-February (DJF, midwinter) and March (late winter) separately for two reasons.
First, the ozone impacts in midwinter are different from those in late winter/early spring, as shortwave effects become important
in spring. Second, our model is biased in March, with too many SSWs compared to reanalysis, a feature also seen in more
recent versions of this model (Gettelman et al., 2019). We see 1.4 March SSWs per decade in NOCHEM and 1.95 March SSWs
per decade in CHEM compared to 0.87-1.1 per decade in the reanalysis (Butler et al., 2017).

130 The stronger vortex in midwinter in the CHEM simulation might lead us to expect fewer DJF SSWs in CHEM than in
NOCHEM. We do see a decrease of about 10% in DJF SSWs with interactive chemistry compared to specified chemistry, but
this decrease is far from being statistically significant. In contrast, in March, we see more SSWs in CHEM than in NOCHEM,
potentially related to the later breakdown of the vortex.

Haase and Matthes (2019) consider the overall (November-March) number of SSWs. They report a decrease in overall SSWs
135 of around 30%. In contrast, for November-March, we find a slight increase in SSWs of about 2% (from 109 events to 111, not
shown) from prescribed chemistry to interactive chemistry.

We now consider SPV frequency. The increase in DJF SPV frequency from NOCHEM to CHEM is about 29%. This is
unsurprising given the stronger vortex in CHEM overall. With our definition of SPVs, the number of March strong vortex events
(in either simulation) is too small for a robust statistical analysis. This is because of the weaker vortex in March compared to
140 DJF; a much larger anomalous vortex strength would be necessary to reach 48 m/s. Because of the low number of such events,
we do not further study March SPVs and thus discard them from the analysis.

We now examine DJF SSWs, March SSWs, and DJF SPVs separately in each of the following three sections.

3.2 Midwinter sudden stratospheric warmings

We start by focusing on the surface impacts of SSWs, seeking to document any differences between the CHEM and NOCHEM
145 simulations. After noting the impact of the events on the surface, we then consider how any differences in those impacts arise
aloft.

Figure 3 shows composite surface level pressure anomalies in the first and second months (top and bottom respectively)
following December-February SSWs in CHEM (left, 75 events) and NOCHEM (middle, 67 events), as well as the difference
between the two (right). We see a strong and significant pattern resembling a negative North Atlantic Oscillation (NAO) in
150 the first month following SSWs in both CHEM and NOCHEM, and in both cases this negative annular mode persists through
the second month following the event. There is minimal difference between the two simulations in the first 30 days, with
the CHEM simulation having only a slightly stronger signal. However, the difference is statistically significant and strongly
projects onto the NAO 30-60 days after the central date. This indicates that the surface signature of SSWs is stronger and more
persistent in CHEM than in NOCHEM.

155 To determine whether these anomalies originate in the stratosphere, we calculate the Northern Annular Mode (NAM) for
CHEM and NOCHEM. We use a method similar to that of Gerber et al. (2010) and Gerber and Martineau (2018); the detailed
procedure is in Appendix A. We show the results of the NAM calculations in Figure 4. The CHEM and NOCHEM composites

around SSWs have comparable NAM anomalies in the stratosphere around the central date, but in the CHEM simulation the negative anomaly persists more strongly in the lower stratosphere beyond 40 days after the central date. The CHEM-NOCHEM

160 difference shows that this change in persistence with interactive chemistry is significant at the 95% level. There is also more descent of the anomaly to the surface in the CHEM simulation, especially at about 30 days after the central date.

This difference in descent is also seen in the CHEM-NOCHEM temperature anomalies (Figure 5 top left). The warming in the stratosphere associated with the onset of the SSW is larger with interactive chemistry. This stratospheric temperature anomaly then descends more strongly through the stratosphere and troposphere in the CHEM simulation than in the NOCHEM

165 simulation.

We investigate the processes leading to these changes in more detail by examining the dynamical, longwave, and shortwave heating terms. The greater warming throughout the stratosphere is due to increased dynamical heating (top right) in CHEM compared to NOCHEM, perhaps because of greater wave activity necessary for an SSW to occur with a stronger mean vortex state, as the higher temperature with interactive chemistry is also associated with a longwave cooling response (bottom left).

170 The higher stratospheric tempertaures result in greater longwave emission. The increase in dynamical forcing also corresponds to increased ozone transport. Ozone is a longwave emitter, so the increased dynamical forcing could directly account for part of this longwave cooling difference, as well.

In DJF, dynamical heating and longwave heating are the dominant temperature tendency terms. There is also a significant shortwave heating response (bottom right), but in midwinter it is an order of magnitude smaller than the other terms, owing to

175 the absence of incoming solar radiation to polar night. The importance of the shortwave response increases the later in winter the SSW events occurs. We illustrate this in Figure 6, showing the difference in shortwave anomalies between CHEM and NOCHEM for SSWs occurring in December, January, and February separately. There is very little difference in shortwave heating anomalies in CHEM compared to NOCHEM for December SSWs, with no difference greater than 0.05 K/day. The difference increases in January, with differences between 0.125 and 0.15 K/day in the upper stratosphere 20-30 days after

180 the central date, but this is still small compared to the dynamical heating and longwave terms. Much stronger differences are seen for February SSWs, with CHEM-NOCHEM differences throughout the upper stratosphere following the central date of comparable magnitude to the differences in longwave heating anomalies of approximately 0.3 K/day.

Finally, we examine the anomaly in total ozone column around the central date of the SSW (Figure 7) in the CHEM simulation. The figure also shows the zonal mean zonal wind to illustrate the corresponding evolution of the vortex. We see a sharp

185 increase in ozone in the 15 days leading up to the central date, reaching a peak of on average about 40 Dobson units above climatology just after the central date, similar to that seen in reanalysis by De La Cámara et al. (2018). This ozone anomaly results from transport due to the greater dynamical forcing in CHEM noted earlier. Following the central date, anomalies of about 20 Dobson units persist for up to 3 months following the central date. This ozone anomaly is consistent with total ozone column in reanalysis reported by De La Cámara et al. (2018) and the smaller ozone depletion in years with early SSWs observed by

190 Strahan et al. (2016).

3.3 March sudden stratospheric warmings

We now turn to the March SSWs. Figure 8 shows the composite sea level pressure anomalies for CHEM and NOCHEM, as well as the CHEM-NOCHEM difference, for each of the first two months following the central date. Both simulations again show a negative NAO-like pattern in the two months following the SSW. There are some regions with significant difference between CHEM and NOCHEM in the first thirty days, but the pattern does not project strongly onto the NAO. Also, there is very little difference between the two composites in the second thirty days after the central date.

The surface responses seen following March SSWs, in both models, are weaker and less persistent than those following DJF SSWs, and the areas of strong or significant low or high anomalies are smaller. This indicates either weaker SSWs than in DJF or weaker stratosphere-troposphere coupling. The differences between surface impacts of SSWs in CHEM and NOCHEM are also weaker for March SSWs. Thus, ozone chemistry seems much less important for the surface effects of March SSWs than for DJF SSWs.

Considering the NAM in these simulations as shown in Figure 9, we see negative NAM anomalies at the surface in both the CHEM and NOCHEM simulations, consistent with the negative NAO-like pattern seen in the Figure 8. There is a stronger signal in the troposphere in the CHEM compared to NOCHEM March SSW simulations at around 15-20 days after the central date, which may correspond to the surface pressure differences.

As for the surface plots, the NAM anomalies again suggest that March SSWs in both CHEM and NOCHEM are weaker overall than the DJF SSWs; the stratospheric NAM anomalies are smaller and less significant. Stratosphere-troposphere coupling also seems weaker compared to that seen for DJF SSWs. Further, the difference in this descent between CHEM and NOCHEM is less strong and persistent than the difference in NAM signals seen in the troposphere after midwinter SSWs.

Soon after the central date for March SSWs, the NAM signal in the stratosphere is weaker with interactive chemistry than with specified chemistry, in contrast to the midwinter SSW case. This difference appears to arise from the temperature and heating anomalies (Figure 10). The lower stratosphere is only briefly and weakly warmer in CHEM compared to NOCHEM. Shortwave heating seems to be dominant in the temperature response to March SSWs, with the CHEM-NOCHEM difference in temperature anomalies (Figure 10a) largely following the difference in shortwave heating anomalies (Figure 10d). This is in contrast to the DJF SSWs, where the shortwave heating had little effect, and dynamical heating was dominant.

Finally, we note that unlike the DJF SSW case, the ozone anomaly for March SSWs does not persist after the event (Figure 11). This is related to the seasonal breakdown of the vortex, seen in the wind curve. Because these are late winter SSWs, the second month following the central date is near the expected stratospheric final warming date; in our simulations, the winds return to easterly about 50 days on average after the March SSW central date. The ozone anomaly returns to 0 Dobson units as the vortex breaks down. The maximum ozone anomaly is also about half the size of the maximum anomaly seen in DJF, consistent with the weaker nature of the events overall.

3.4   Midwinter strong polar vortex events

Finally, we turn our attention to strong polar vortex (SPV) events in DJF. While less extensively studied than SSWs, SPVs also impact surface climate. Baldwin and Dunkerton (2001) suggest that strong polar vortex events can have surface signals

225   comparable to but opposite in sign to those following SSWs, and Smith et al. (2018) found effects of Northern Hemisphere SPVs on spring and summer Arctic sea ice.

In the thirty days following the SPV central date, we see a pattern reminiscent of a weakly positive NAO in both CHEM and NOCHEM (Figure 12). This positive NAO-like pattern appears stronger in CHEM than in NOCHEM, but not significantly so. There is very little difference from climatology at the surface in the second month after the event in either of the simulations.

230   The NAM anomalies following SPVs in CHEM and NOCHEM (Figure 13) have similar strength (and opposite sign) in the stratosphere to those following midwinter SSWs, but they have much weaker downward propagation, consistent with an only weakly positive NAO. The difference between the NAM anomalies in CHEM and NOCHEM confirms a more positive NAM in mid-to-lower troposphere in the first month following the SPV central date with interactive chemistry, but again, this difference is not significant and does not reach the surface.

235   These minimal differences in surface pressure and NAM are consistent with the lack of differences in stratospheric temperature and temperature tendencies, shown in Figure 14. A small shortwave heating difference is expected in midwinter, but the longwave and dynamical heating differences are also much smaller than for midwinter SSWs. The only large and significant difference in stratospheric temperature is 40-60 days following the SPV central date, when the stratosphere is colder with interactive chemistry. This is after zonal mean zonal winds have returned to typical levels and is thus likely related to the stronger

240   mean state of the stratospheric polar vortex with interactive chemistry compared to specified chemistry. However, this does not affect the surface.

We also see a weaker ozone anomaly following SPVs than following SSWs, with a maximum anomaly of about 30 Dobson units compared to 40 (Figure 15). The ozone decrease following SPVs is also much more gradual than the increase seen in DJF SSWs. This is consistent with the fact that SPVs are not strong and sudden dynamical events in the way that SSWs are.

245   As with DJF SSWs, though, the anomaly does persist for three months after the central date.

4   Conclusions

The climate model results presented here show an important contribution of interactive ozone chemistry to the climatological state of the stratospheric polar vortex and to the Euro-Atlantic surface impacts of midwinter SSWs. However, ozone chemistry has minimal impact on the surface effects of March SSWs and of midwinter SPVs, despite long-lasting total ozone column

250   anomalies in the latter case. Furthermore, in contrast to the results reported by Haase and Matthes (2019), we do not find significantly fewer SSWs with interactive chemistry, despite the stronger climatological polar vortex. We do find more frequent SPVs, however.

The stronger polar vortex mean state with interactive ozone chemistry also affects the surface signature of SSWs. Stronger wave forcing is necessary for an SSW to occur, and the resulting negative NAM propagates to the surface more strongly, as well.

255 This result is also consistent with that reported by Haase and Matthes (2019), though the effects documented here are weaker. In extending this work to consider March SSWs, we found that while the same stronger dynamical forcing is present, the influence of the shortwave heating term in late winter/early spring results in a stratospheric temperature difference of opposite sign, and with little difference at the surface following March SSWs between interactive chemistry and specified chemistry simulations. We also find minimal impact on midwinter surface effects of SPVs; the negative ozone anomalies associated with

260 SPVs instead have an effect in spring (Ivy et al., 2017).

Previous work (Smith and Polvani, 2014; Calvo et al., 2015; Ivy et al., 2017; Lin et al., 2017; Rieder et al., 2019) has shown the importance of ozone for the stratospheric polar vortex and surface springtime climate variability. Haase and Matthes (2019) further suggested that feedbacks among chemistry and dynamics are important for accurately capturing response at the surface to SSWs, one of the major drivers of North Atlantic and European winter climate variability. By running longer

265 simulations allowing for a clean quantification of the impact of interactive ozone, we find that these feedbacks are important for representing impacts of midwinter SSWs. However, we do not find similar importance for describing surface response to March SSWs or DJF SPVs. Our results suggest that including interactive ozone chemistry may have a sizable impact on N.Atlantic and European winter and spring climate variability in models.

Finally, we note that while we have only focused on winter SSWs and SPVs, stratospheric final warmings also have tro-

270 pospheric effects (Black et al., 2006; Ayarzagüena and Serrano, 2009; Wei et al., 2007; Hardiman, 2011; Thieblemont et al., 2019; Butler et al., 2019). Those effects are dependent on the timing of the final warming, with earlier final warmings resulting in surface effects more like those seen following SSWs (Ayarzagüena and Serrano, 2009; Li et al., 2012). Interactive chemistry may thus also affect the representation and surface signature of stratospheric final warmings in models; this will be investigated in a follow-up study.

Author contributions. GC and LMP designed the model experiment. JO, GC, and LMP decided on the analysis, and wrote the paper. GC carried out the model simulations. JO performed the data analysis and produced the figures.

Competing interests. The authors declare that they have no conflict of interest.

Appendix A

We calculate the NAM using a method similar to that of Gerber et al. (2010) and Gerber and Martineau (2018). The specific
procedure is as follows:

1. We average model output to find a time series of daily, zonal mean geopotential height $Z(t, \lambda, p)$ as a function of time t,
   latitude λ, and pressure p.

2. For every day and pressure level, we remove the global mean geopotential height $\bar{Z}^{\mathrm{global}}(t, p)$. This helps to remove the
   global changes so that the index instead mainly captures meridional differences or shifts (Gerber et al., 2010). (While
   not the case for the simulations used in this study, this step would remove much of the global warming signal if it were
   present.)

3. For each day, latitude, and pressure level, we remove the average for that calendar day over the whole period; that is, we
   remove the climatology to find an anomalous height.

4. For each day, latitude, and pressure, we remove the linear trend over the period.

5. For each day and pressure level, we compute a polar cap average. Here we are interested in the NAM, and we take the
   average from 65-90°N. This is a proxy for the annular mode as shown in Baldwin and Thompson (2009).

6. We multiply by -1 so that a positive polar cap geopotential height anomaly yields a negative NAM, for consistency with
   the convention of Thompson and Wallace (1998).

7. We normalize the index by its standard deviation at each pressure level.

References

Ayarzagüena, B. and Serrano, E.: Monthly Characterization of the Tropospheric Circulation over the Euro-Atlantic Area in Relation with the Timing of Stratospheric Final Warmings, Journal of Climate, 22, 6313–6324, https://doi.org/10.1175/2009JCLI2913.1, 2009.

Baldwin, M. P. and Dunkerton, T. J.: Stratospheric Harbingers of Anomalous Weather Regimes, Science, 294, 581–584, https://doi.org/10.1126/science.1063315, http://www.sciencemag.org/cgi/doi/10.1126/science.1063315, 2001.

Baldwin, M. P. and Thompson, D. W.: A critical comparison of stratosphere-troposphere coupling indices, Quarterly Journal of the Royal Meterological Society, 135, 1661–1672, 2009.

Beerli, R. and Grams, C. M.: Stratospheric modulation of the large-scale circulation in the Atlantic-European region and its implications for surface weather events, Quarterly Journal of the Royal Meteorological Society, https://doi.org/10.1002/qj.3653, 2019.

Black, R. X., McDaniel, B. A., and Robinson, W. A.: Stratosphere-Troposphere coupling during spring onset, Journal of Climate, 19, 4891–4901, https://doi.org/10.1175/JCLI3907.1, 2006.

Butler, A. H. and Gerber, E. P.: Optimizing the Definition of a Sudden Stratospheric Warming, Journal of Climate, 31, 2337–2344, https://doi.org/10.1175/JCLI-D-17-0648.1, http://journals.ametsoc.org/doi/10.1175/JCLI-D-17-0648.1, 2018.

Butler, A. H., Sjoberg, J. P., Seidel, D. J., and Rosenlof, K. H.: A sudden stratospheric warming compendium, Earth System Science Data, 9, 63–76, https://doi.org/10.5194/essd-9-63-2017, 2017.

Butler, A. H., Charlton-Perez, A., Domeisen, D. I. V., Simpson, I. R., and Sjoberg, J.: Predictability of Northern Hemisphere Final Stratospheric Warmings and Their Surface Impacts, Geophysical Research Letters, 46, 10 578–10 588, https://doi.org/10.1029/2019GL083346, 2019.

Calvo, N., Polvani, L. M., and Solomon, S.: On the surface impact of Arctic stratospheric ozone extremes, Environmental Research Letters, 10, 094 003, https://doi.org/10.1088/1748-9326/10/9/094003, http://stacks.iop.org/1748-9326/10/i=9/a=094003?key=crossref. dab5dcc8df2c81f8936a64f51ce43550, 2015.

Charlton, A. J. and Polvani, L. M.: A New Look at Stratospheric Sudden Warmings. Part I: Climatology and Modeling Benchmarks, Journal of Climate, 20, 449–469, https://doi.org/10.1175/JCLI3996.1, http://journals.ametsoc.org/doi/abs/10.1175/JCLI3996.1, 2007a.

Charlton, A. J. and Polvani, L. M.: A New Look at Stratospheric Sudden Warmings. Part II: Evaluation of Numerical Modeling Simulations, Journal of Climate, 20, 470–488, https://doi.org/10.1175/JCLI3994.1, 2007b.

Charlton-Perez, A. J. and Polvani, L. M.: CORRIGENDUM, Journal of Climate, 24, 5951–5951, https://doi.org/10.1175/JCLI-D-11-00348.1, http://journals.ametsoc.org/doi/abs/10.1175/JCLI-D-11-00348.1, 2011.

De La Cámara, A., Abalos, M., Hitchcock, P., Calvo, N., and Garcia, R. R.: Response of Arctic ozone to sudden stratospheric warmings, Atmospheric Chemistry and Physics, 18, 16 499–16 513, https://doi.org/10.5194/acp-18-16499-2018, https://www.atmos-chem-phys.net/18/16499/2018/, 2018.

Gerber, E. P. and Martineau, P.: Quantifying the variability of annular modes: reanalysis uncertainty vs. sampling uncertainty, Atmospheric Chemistry and Physics, 18, 17 099–17 117, https://doi.org/10.5194/acp-18-17099-2018, 2018.

Gerber, E. P., Baldwin, M. P., Akiyoshi, H., Austin, J., Bekki, S., Braesicke, P., Butchart, N., Chipperfield, M., Dameris, M., Dhomse, S., Frith, S. M., Garcia, R. R., Garny, H., Gettelman, A., Hardiman, S. C., Karpechko, A., Marchand, M., Morgenstern, O., Nielsen, J. E., Pawson, S., Peter, T., Plummer, D. A., Pyle, J. A., Rozanov, E., Scinocca, J. F., Shepherd, T. G., and Smale, D.: Stratosphere-troposphere coupling and annular mode variability in chemistry-climate models, Journal of Geophysical Research: Atmospheres, 115, https://doi.org/10.1029/2009JD013770, https://agupubs.onlinelibrary.wiley.com/doi/abs/10.1029/2009JD013770, 2010.

Gettelman, A., Mills, M. J., Kinnison, D. E., Garcia, R. R., Smith, A. K., Marsh, D. R., Tilmes, S., Vitt, F., Bardeen, C. G., McInerney, J., Liu, H.-L., Solomon, S. C., Polvani, L. M., Emmons, L. K., Lamarque, J.-F., Richter, J. H., Glanville, A. S., Bacmeister, J. T., Phillips, A. S., Neale, R. B., Simpson, I. R., DuVivier, A. K., Hdzic, A., and Randel, W. J.: The Whole Atmosphere Community Climate Model

340   Version 6 (WACCM6), Journal of Geophysical Research Atmospheres, https://doi.org/10.1029/2019JD030943, 2019.

Haase, S. and Matthes, K.: The importance of interactive chemistry for stratosphere–troposphere coupling, Atmospheric Chemistry and Physics, 19, 3417–3432, https://doi.org/10.5194/acp-19-3417-2019, https://www.atmos-chem-phys.net/19/3417/2019/, 2019.

Hardiman, S. C. e. a.: Improved predictability of the troposphere using stratospheric final warmings, Journal of Geophysical Research Atmospheres, 116, D18 113, https://doi.org/10.1029/2011JD015914, 2011.

345 Ivy, D. J., Solomon, S., Calvo, N., and Thompson, D. W. J.: Observed connections of Arctic stratospheric ozone extremes to Northern Hemisphere surface climate, Environmental Research Letters, 12, 024 004, https://doi.org/10.1088/1748-9326/aa57a4, http://stacks.iop. org/1748-9326/12/i=2/a=024004?key=crossref.8bb0b7585b138903acc96d5787953e21, 2017.

Karpechko, A. Y., Perlwitz, J., and Manzini, E.: A model study of the tropospheric impacts of the Arctic ozone depletion of 2011, Journal of Geophysical Research, 119, 7999–8014, https://doi.org/10.1002/2013JD021350, 2014.

350 Kinnison, D. E., Brasseur, G. P., Walters, S., Garcia, R. R., Marsh, D. R., Sassi, F., Harvey, V. L., Randall, C. E., Emmons, L., Lamarque, J. F., Hess, P., Orlando, J. J., Tie, X. X., Randel, W., Pan, L. L., Gettelman, A., Granier, C., Diehl, T., Niemeier, U., and Simmons, A. J.: Sensitivity of chemical tracers to meteorological parameters in the MOZART-3 chemical transport model, Journal of Geophysical Research Atmospheres, 112, D20 302, https://doi.org/10.1029/2006JD007879, 2007.

Li, L., Li, C., Pan, J., and Tan, Y.: On the differences and climate impacts of early and late stratospheric polar vortex breakup, Advances in

355   Atmospheric Sciences, 29, 1119–1128, https://doi.org/10.1007/s00376-012-1012-4, 2012.

Limpasuvan, V., Thompson, D. W. J., and Hartmann, D. L.: The Life Cycle of the Northern Hemisphere Sudden Stratospheric Warmings, Journal of Climate, 17, 2584–2596, 2004.

Limpasuvan, V., Hartmann, D. L., Thompson, D. W. J., Jeev, K., and Yung, Y. L.: Stratosphere-troposphere evolution during polar vortex intensification, Journal of Geophysical Research Atmospheres, 110, D24 101, https://doi.org/10.1029/2005JD006302, 2005.

360 Lin, P., Paynter, D., Polvani, L., Correa, G. J. P., Ming, Y., and Ramaswamy, V.: Dependence of model-simulated response to ozone depletion on stratospheric polar vortex climatology: RESPONSE TO OZONE DEPENDS ON CLIMATOLOGY, Geophysical Research Letters, 44, 6391–6398, https://doi.org/10.1002/2017GL073862, http://doi.wiley.com/10.1002/2017GL073862, 2017.

Marsh, D. R., Mills, M. J., Kinnison, D. E., Lamarque, J.-F., Calvo, N., and Polvani, L. M.: Climate Change from 1850 to 2005 Simulated in CESM1(WACCM), Journal of Climate, 26, 7372–7391, https://doi.org/10.1175/JCLI-D-12-00558.1, http://journals.ametsoc.org/doi/abs/

365   10.1175/JCLI-D-12-00558.1, 2013.

Previdi, M. and Polvani, L. M.: Climate system response to stratospheric ozone depletion and recovery, Quarterly Journal of the Royal Meteorological Society, 140, 2401–2419, https://doi.org/10.1002/qj.2330, 2014.

Rieder, H. E., Chiodo, G., Fritzer, J., Wienerroither, C., and Polvani, L. M.: Is interactive ozone chemistry important to represent polar cap stratospheric temperature variability in Earth-System Models?, Environmental Research Letters, 14, 044 026,

370   https://doi.org/10.1088/1748-9326/ab07ff, https://doi.org/10.1088%2F1748-9326%2Fab07ff, 2019.

Scaife, A. A., Karpechko, A. Y., Baldwin, M. P., Brookshaw, A., Butler, A. H., Eade, R., Gordon, M., MacLachlan, C., Martin, N., Dunstone, N., and Smith, D.: Seasonal winter forecasts and the stratosphere, Atmospheric Science Letters, 17, 51–56, https://doi.org/10.1002/asl.598, 2016.

Smith, K. L. and Polvani, L. M.: The surface impacts of Arctic stratospheric ozone anomalies, Environmental Research Letters, 9, 074 015, https://doi.org/10.1088/1748-9326/9/7/074015, http://stacks.iop.org/1748-9326/9/i=7/a=074015?key=crossref.f94c7a38992e3fe37e21ee98cf969690, 2014.

Smith, K. L., Neely, R. R., Marsh, D. R., and Polvani, L. M.: The Specified Chemistry Whole Atmosphere Community Climate Model (SC-WACCM), Journal of Advances in Modeling Earth Systems, 6, 883–901, https://doi.org/10.1002/2014MS000346, http://doi.wiley.com/10.1002/2014MS000346, 2014.

Smith, K. L., Polvani, L. M., and Tremblay, L. B.: The Impact of Stratospheric Circulation Extremes on Minimum Arctic Sea Ice Extent, Journal of Climate, 31, 7169–7183, https://doi.org/10.1175/JCLI-D-17-0495.1, http://journals.ametsoc.org/doi/10.1175/JCLI-D-17-0495.1, 2018.

Strahan, S. E. and Douglass, A. R.: Evaluating the credibility of transport processes in simulations of ozone recovery using the Global Modeling Initiative three-dimensional model, Journal of Geophysical Research Atmospheres, 109, D05 110, https://doi.org/10.1029/2003JD004238, 2004.

Strahan, S. E., Douglass, A. R., and Steenrod, S. D.: Chemical and Dynamical Impacts of Stratospheric Sudden Warmings on Arctic Ozone Variability, Journal of Geophysical Research Atmospheres, 121, 11 836–11 851, https://doi.org/10.1002/2016JD025128, 2016.

Thieblemont, R., Ayarzaguena, B., Matthes, K., Bekki, S., Abalichin, J., and Langematz, U.: Drivers and Surface Signal of Interannual Variability of Boreal Stratospheric Final Warmings, Journal of Geophysical Research Atmospheres, 124, 5400–5417, https://doi.org/10.1029/2018JD029852, 2019.

Thompson, D. W. J. and Wallace, J. M.: The Arctic Oscillation signature in the wintertime geopotential height and temperature fields, Geophysical Research Letters, 25, 1297–1300, 1998.

Tripathi, O. P., Charlton-Perez, A., Sigmond, M., and Vitart, F.: Enhanced long-range forecast skill in boreal winter following stratospheric strong vortex conditions, Environmental Research Letters, 10, 104 007, https://doi.org/10.1088/1748-9326/10/10/104007, http://stacks.iop.org/1748-9326/10/i=10/a=104007?key=crossref.ca018ccbe2e43e0823d6e4f874940861, 2015.

Wei, K., Chen, W., and Huang, R. H.: Dynamical diagnosis of the breakup of the stratospheric polar vortex in the Northern Hemisphere, Sci. China Ser. D, 50, 1369–1379, https://doi.org/10.1007/s11430-007-0100-2, 2007.
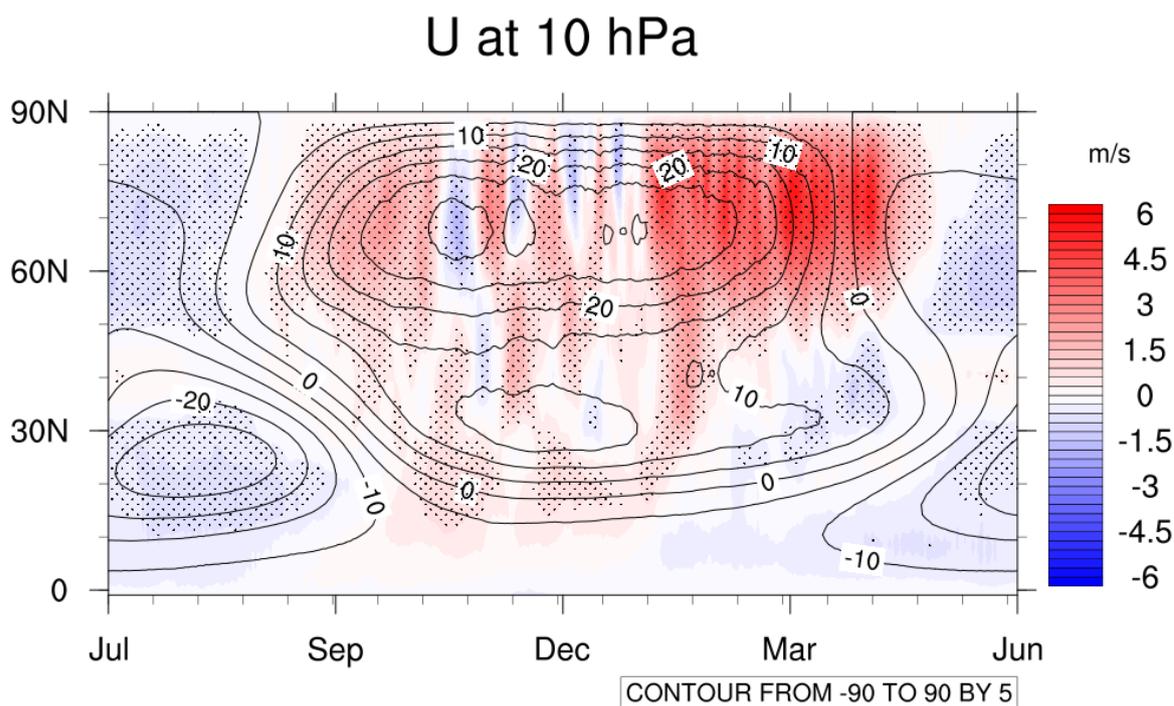
Figure 1. Latitude-time plot of zonal mean zonal wind at 10 hPa. Contours show NOCHEM values in m/s. Colored shading shows the difference CHEM-NOCHEM in m/s. Stippling indicates a significant CHEM-NOCHEM difference at a 95% level using a two-sample two-tailed t-test.
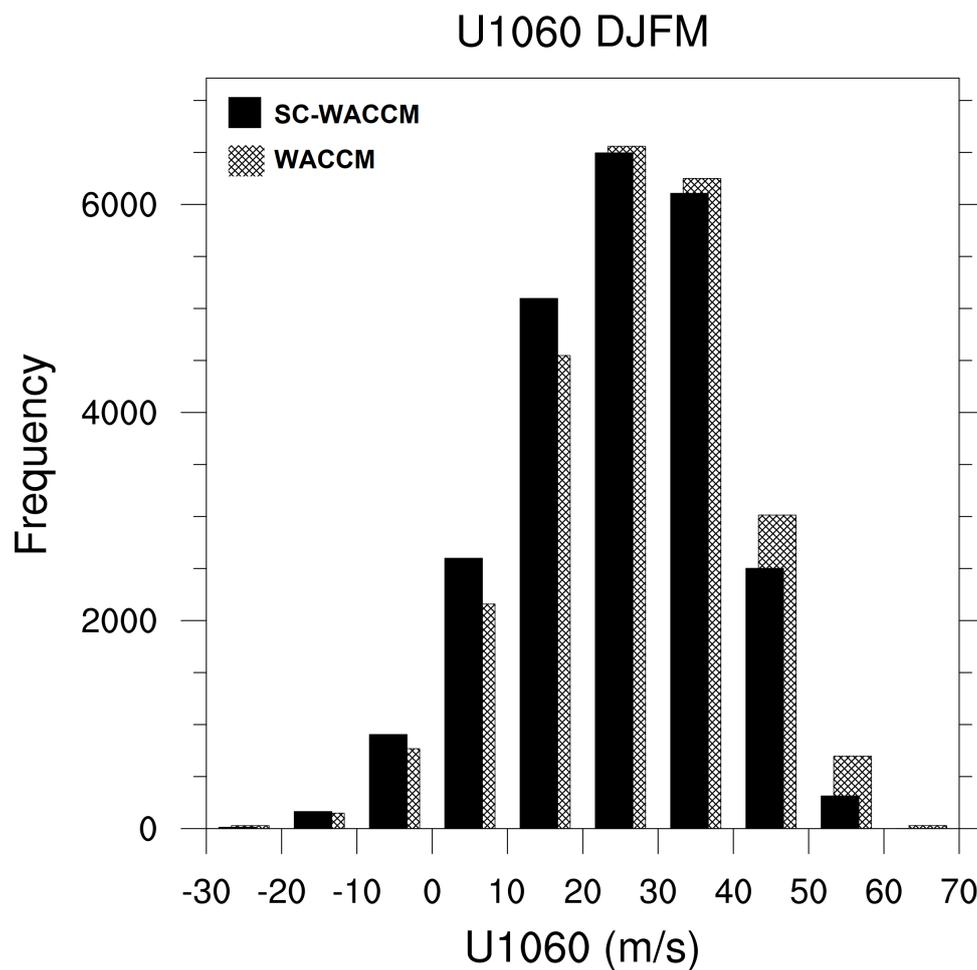
Figure 2. Histogram of daily values of zonal mean zonal wind at 10 hPa and 60°N in December-March for CHEM and NOCHEM. The mean and standard deviation of the CHEM zonal mean zonal wind values are 26.5 m/s and 12.9 m/s. For NOCHEM, these values are 25.0 m/s and 12.3 m/s respectively. The shift to a stronger vortex in CHEM compared to NOCHEM is statistically significant at the 95% level based on a Kolmogorov-Smirnov test; the difference in means is significant at the 95% level based on a two-sample t-test.

	NOCHEM	CHEM	Percent Difference	p-value
Total Winters	200	200		
DJF SSW events	75	67	-10.7%	0.45
DJF SPV events	58	74	+29.3%	0.13
March SSW events	28	39	+39.3%	0.14
March SPV events	7	5	-28.6%	0.58

Table 1. Summary of sudden stratospheric warming (SSW) and strong polar vortex (SPV) events in 200-year year 2000 timeslices with and without interactive chemistry (CHEM and NOCHEM respectively). We separately consider the events occurring in December through February and those occurring in March. Reported p-values are based on a two-tailed two sample t-test (Charlton and Polvani, 2007b).
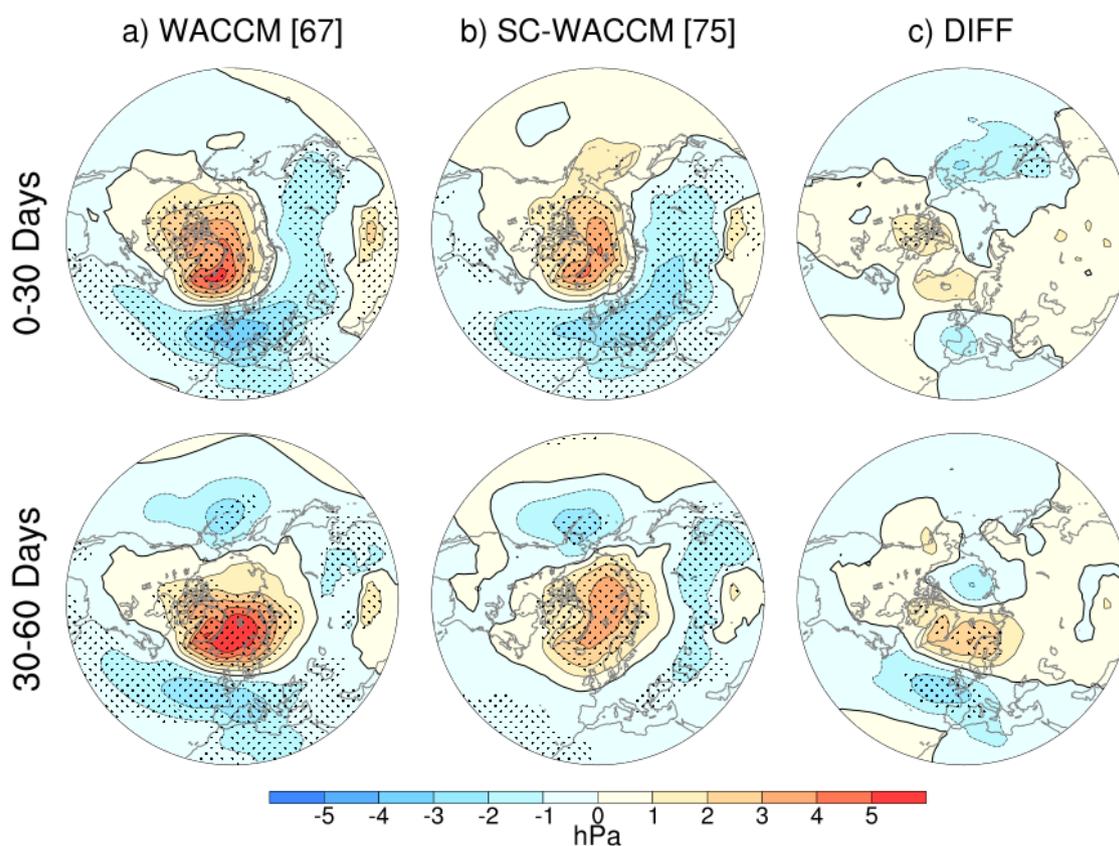
Figure 3. Composites of sea level pressure (SLP) anomalies (in hPa) in the 0-30 and 30-60 days following the central date of DJF SSWs in CHEM (WACCM, a) and NOCHEM (SC-WACCM, b) simulations, as well as the difference in the CHEM and NOCHEM composites (c). Significance at the 95% level using a Monte Carlo test (a,b) or a two-sided t-test (c) is indicated by stippling. The number of events included in each composite is noted in brackets above the figures.
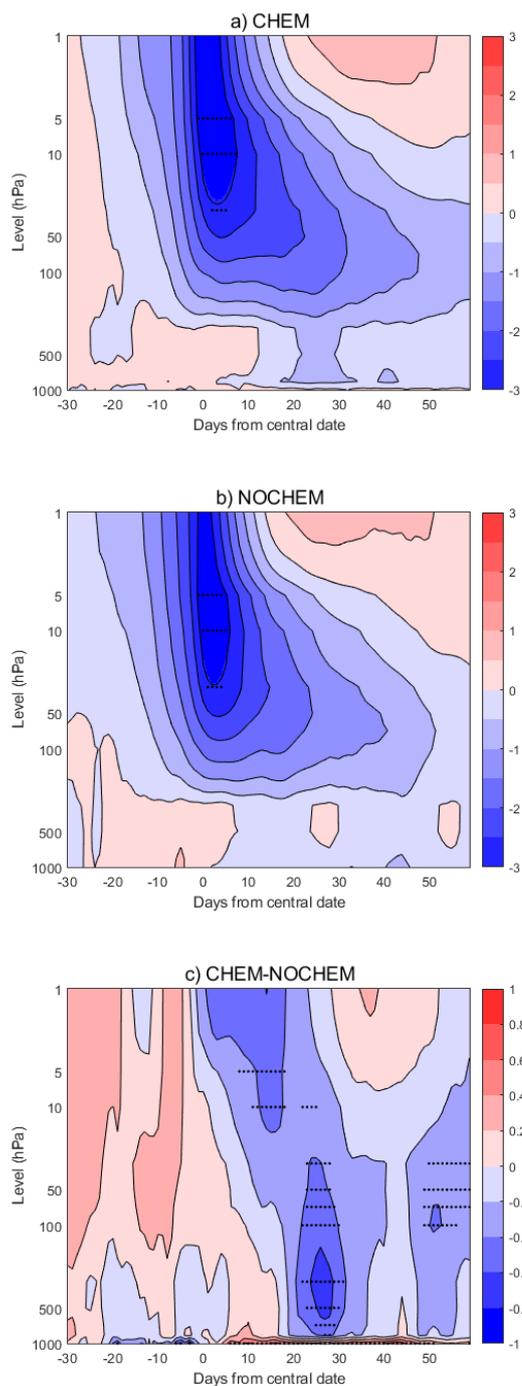
Figure 4. NAM anomaly composites around DJF SSW central dates in CHEM (top), NOCHEM (middle), CHEM-NOCHEM (bottom). Stippling shows significance at the 95% level (with a Monte Carlo test for CHEM and NOCHEM and a two-tailed t-test for CHEM-NOCHEM). Contours are every 0.5 standard units for CHEM and NOCHEM and every 0.2 standard units for CHEM-NOCHEM.
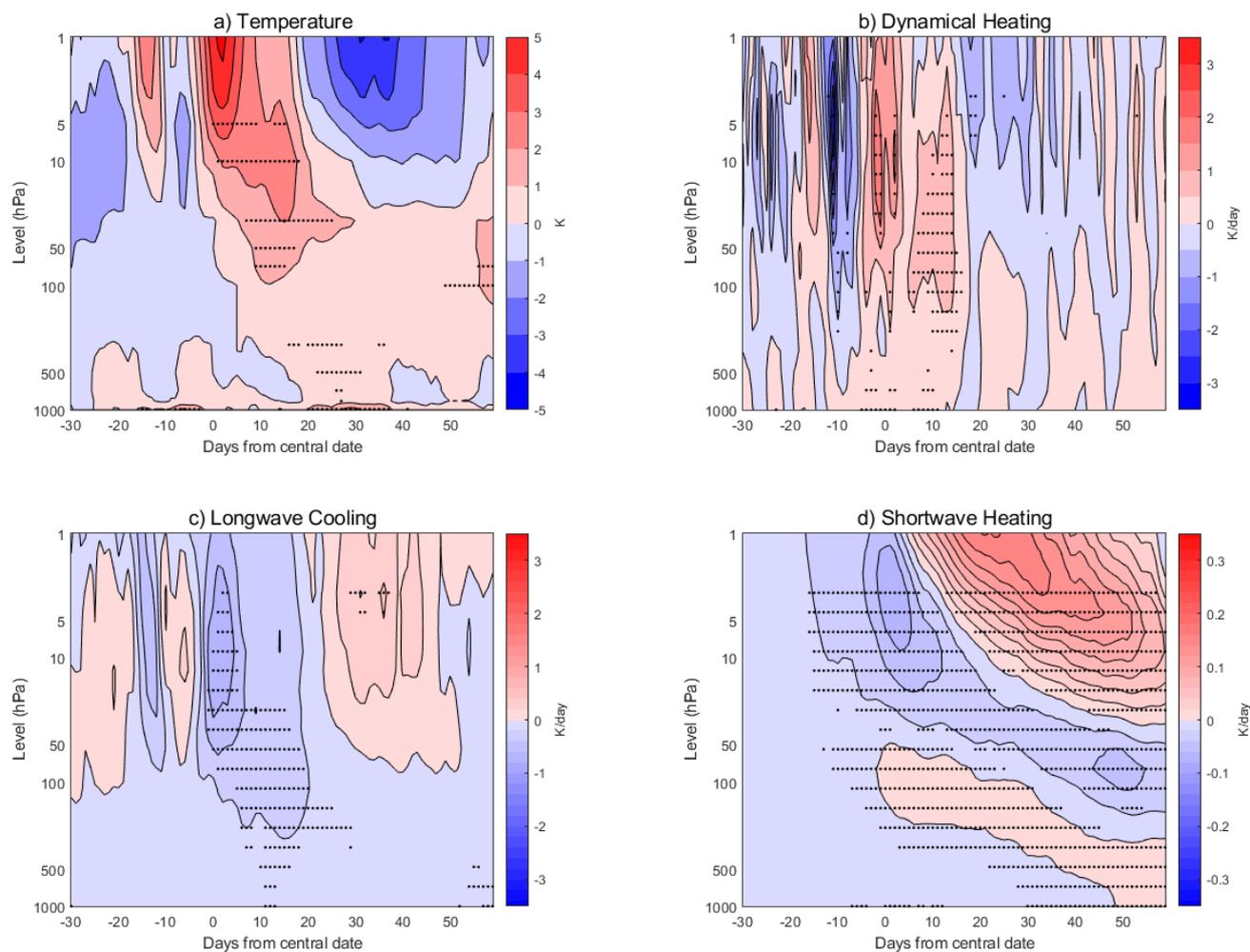
Figure 5. CHEM-NOCHEM differences in the temperature and heating anomalies from -30 to +60 days around the SSW DJF central dates. Top left: temperature anomalies. Contours are every 1 K. Top right: dynamical heating anomalies. Contours are every 0.5 K/day. Bottom left: longwave heating anomalies. Contours are every 0.25 K/day. Bottom right: shortwave heating anomalies. Contours are every 0.02 K/day. Stippling shows significance at the 95% level under a two-tailed t-test.
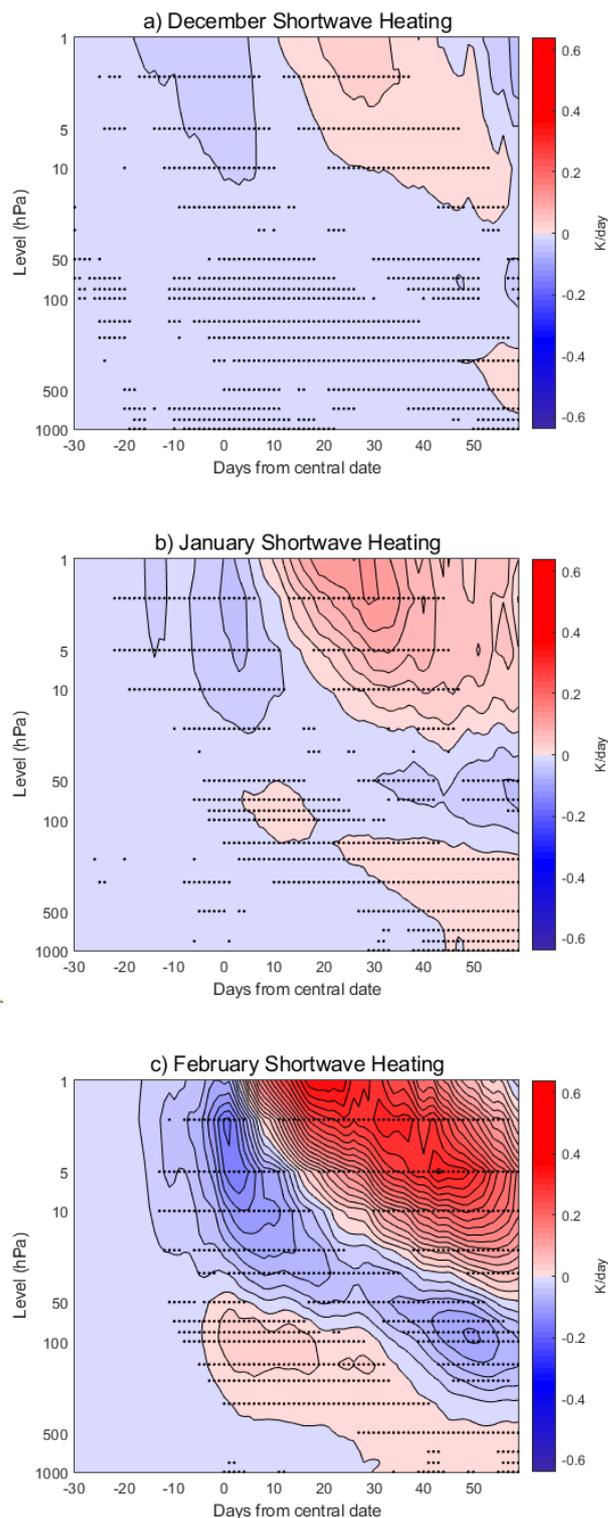
Figure 6. CHEM-NOCHEM difference in shortwave heating anomalies from -30 to +60 days around the SSW central dates in December (top), January (middle), and February (bottom).
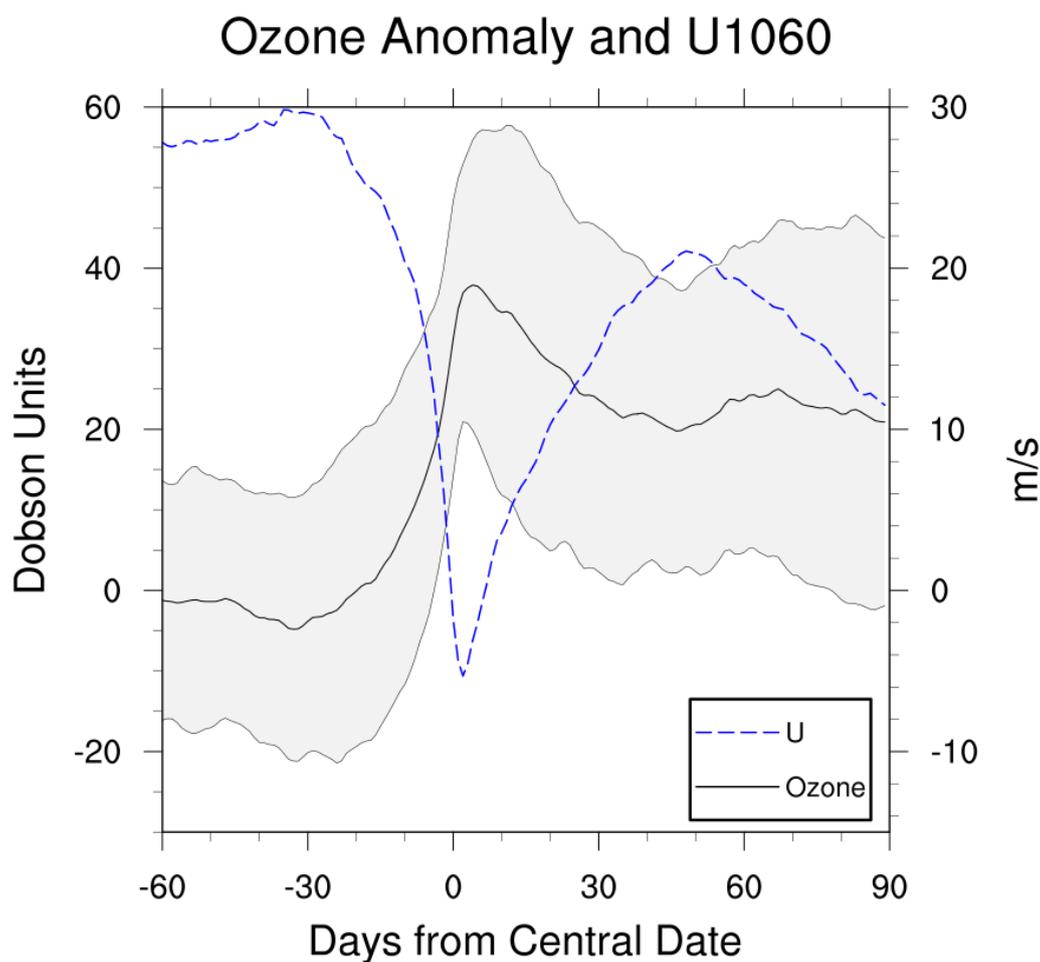
Figure 7. Composite of total column polar cap ozone anomalies in Dobson units and composite of zonal mean zonal wind at 60° N and 10 hPa in m/s from -60 to 90 days around the central date of DJF SSWs in CHEM simulations. The black line shows the mean total ozone column; 1σ from the mean is shaded. The blue dashed line shows the mean U1060.
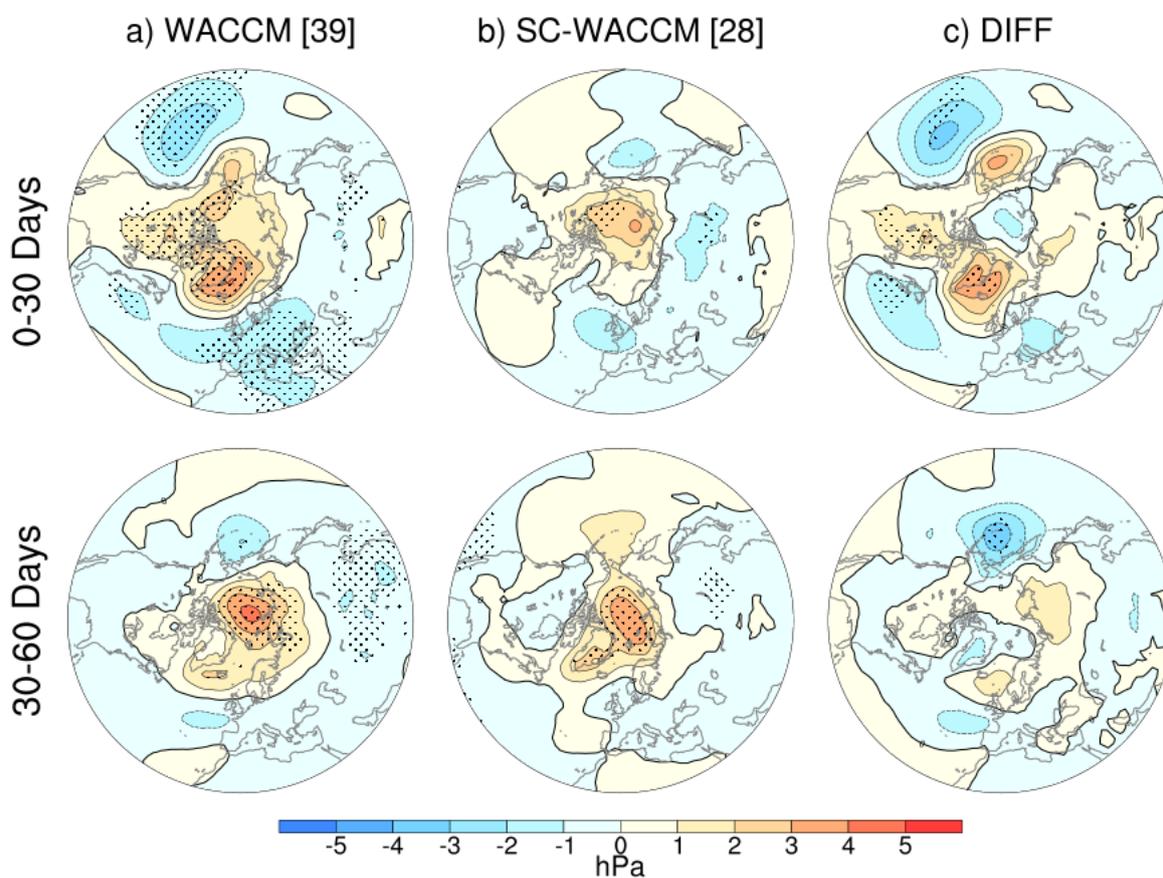
Figure 8. As in Figure 3, for March SSWs.
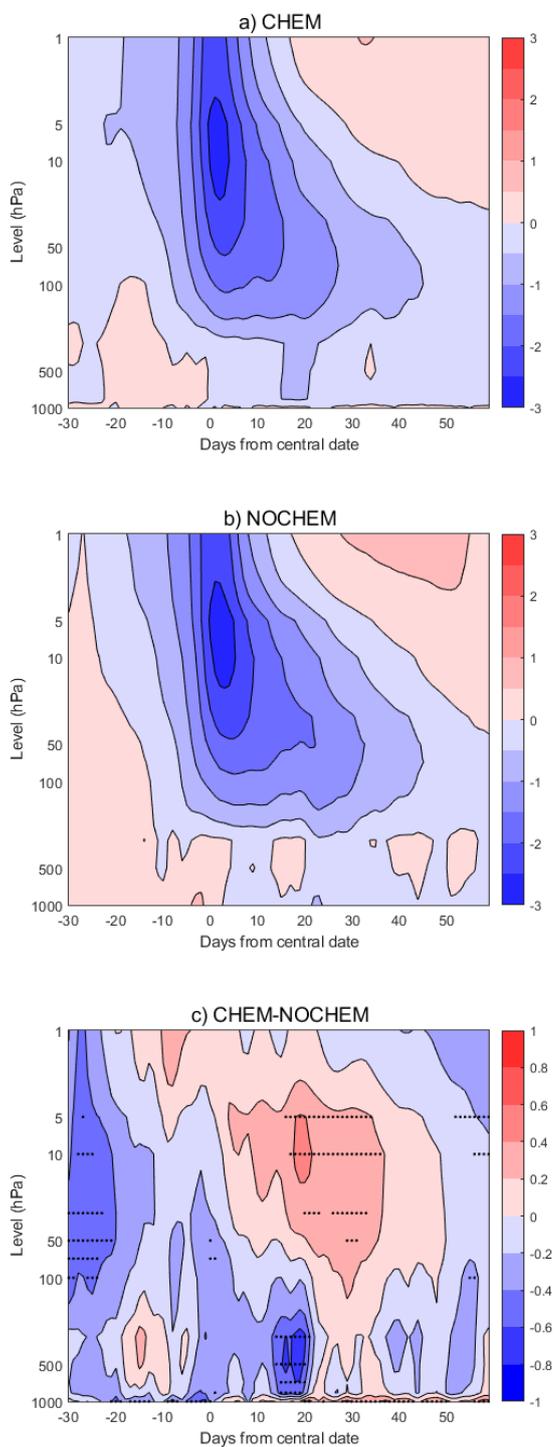
Figure 9. As in Figure 4, for March SSWs.
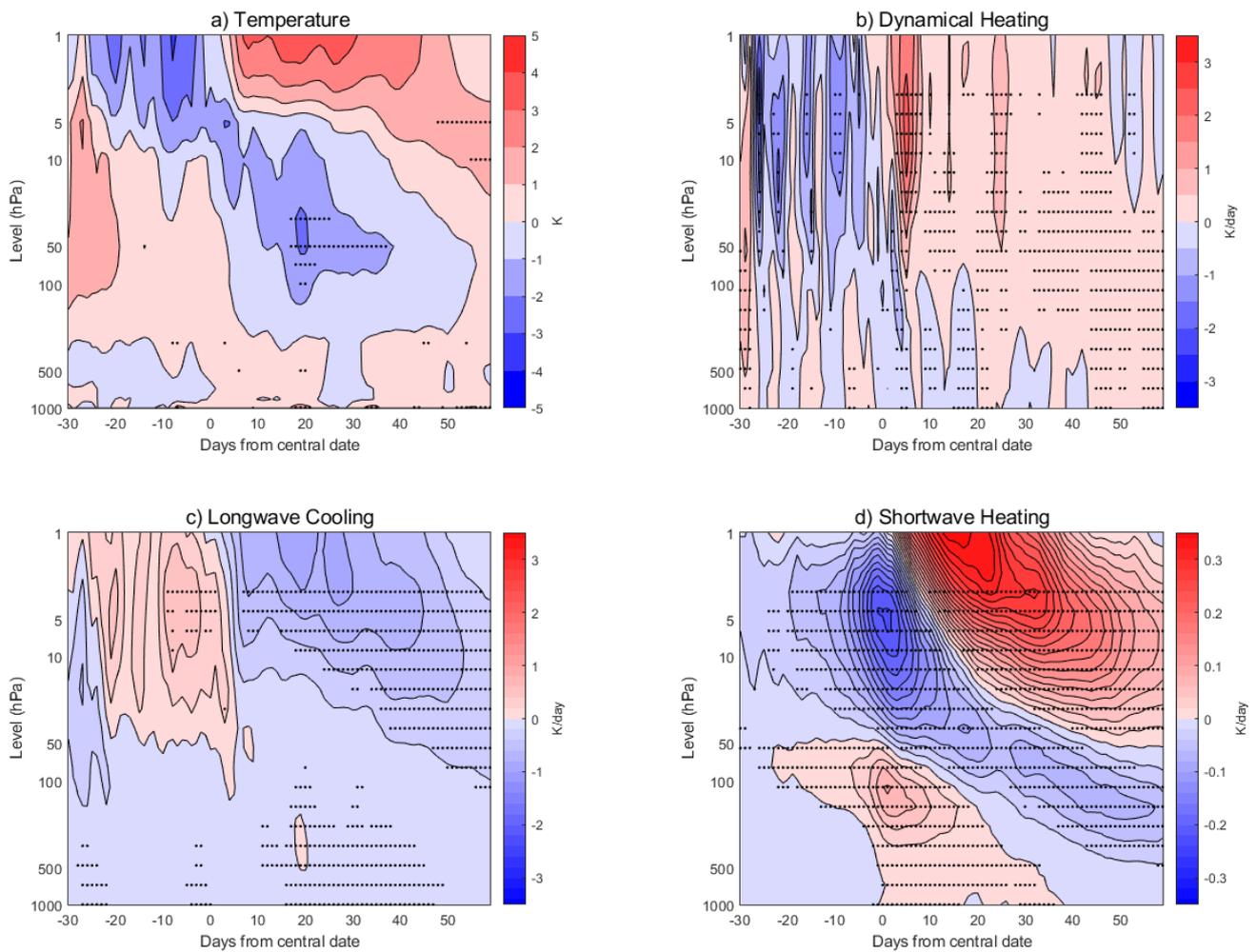
Figure 10. As in Figure 5, for March SSWs.

Atmospheric
Chemistry
and Physics
Discussions

Open Access

EGU
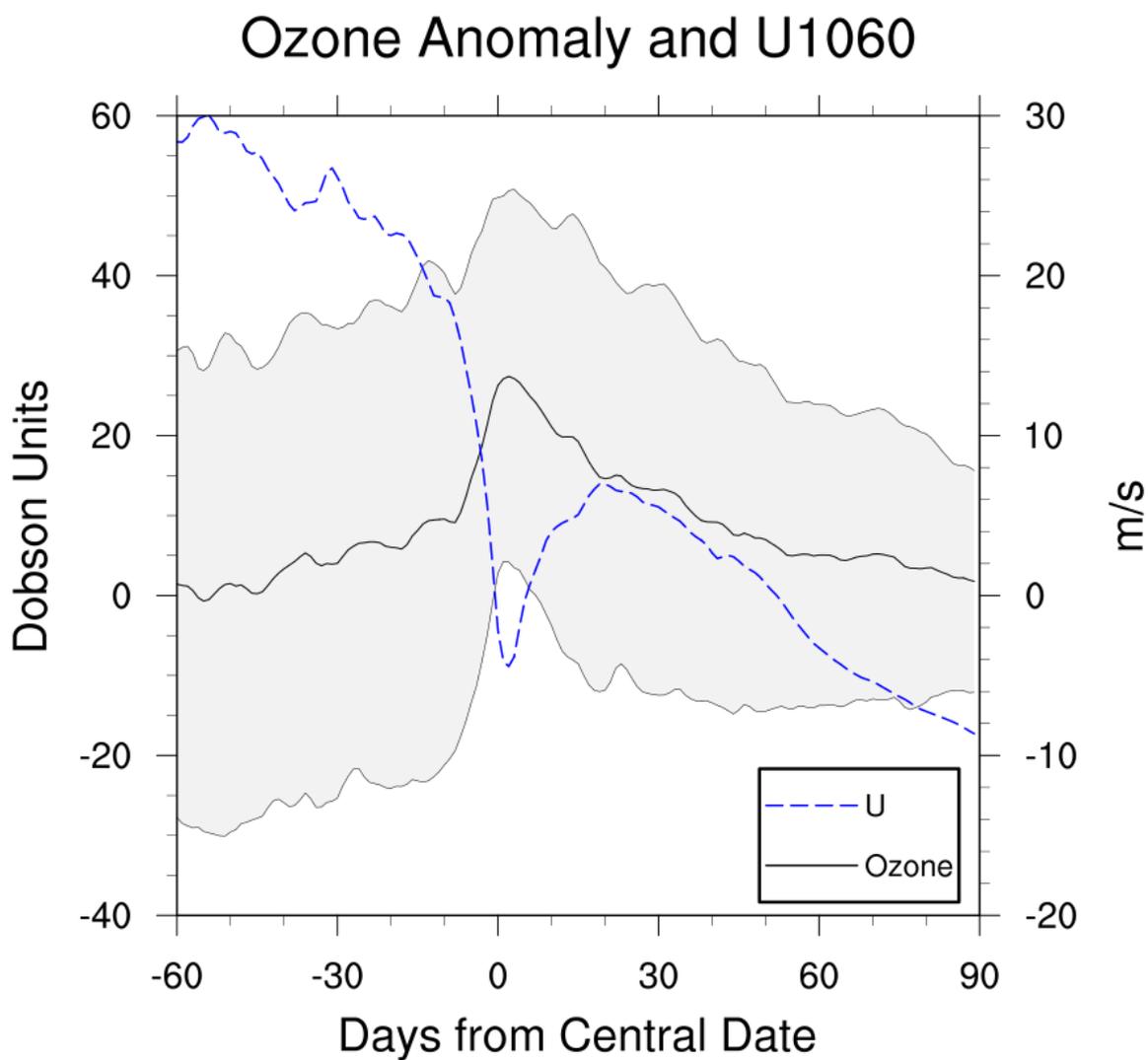
Figure 11. As in Figure 7, for March SSWs.
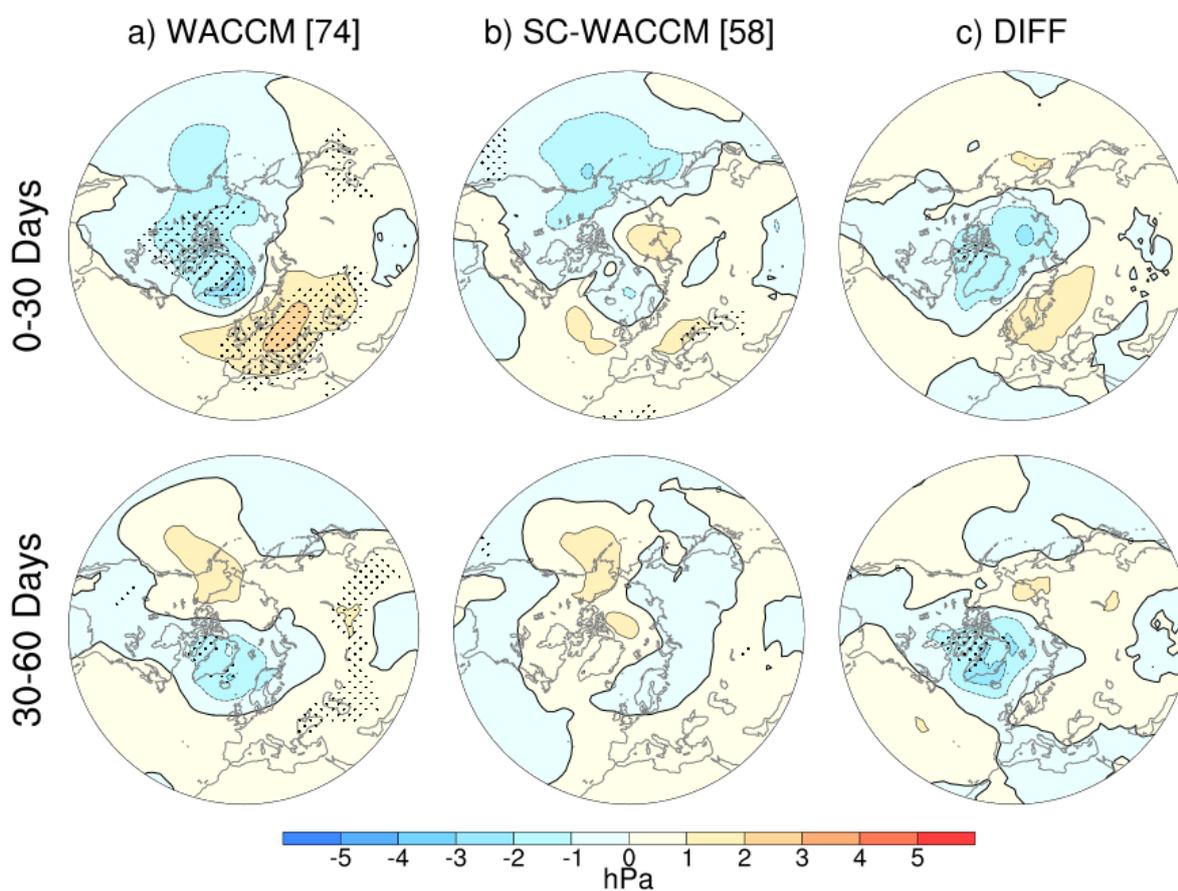
Figure 12. As in Figure 3, for DJF SPVs.
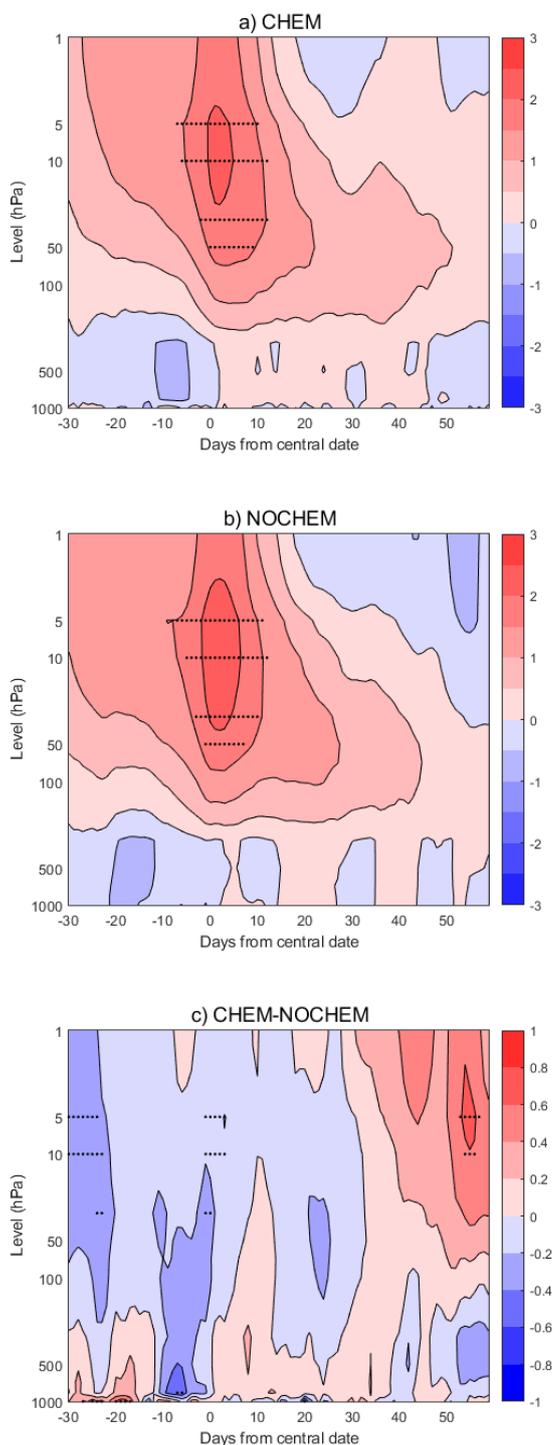
Figure 13. As in Figure 4, for DJF SPVs.
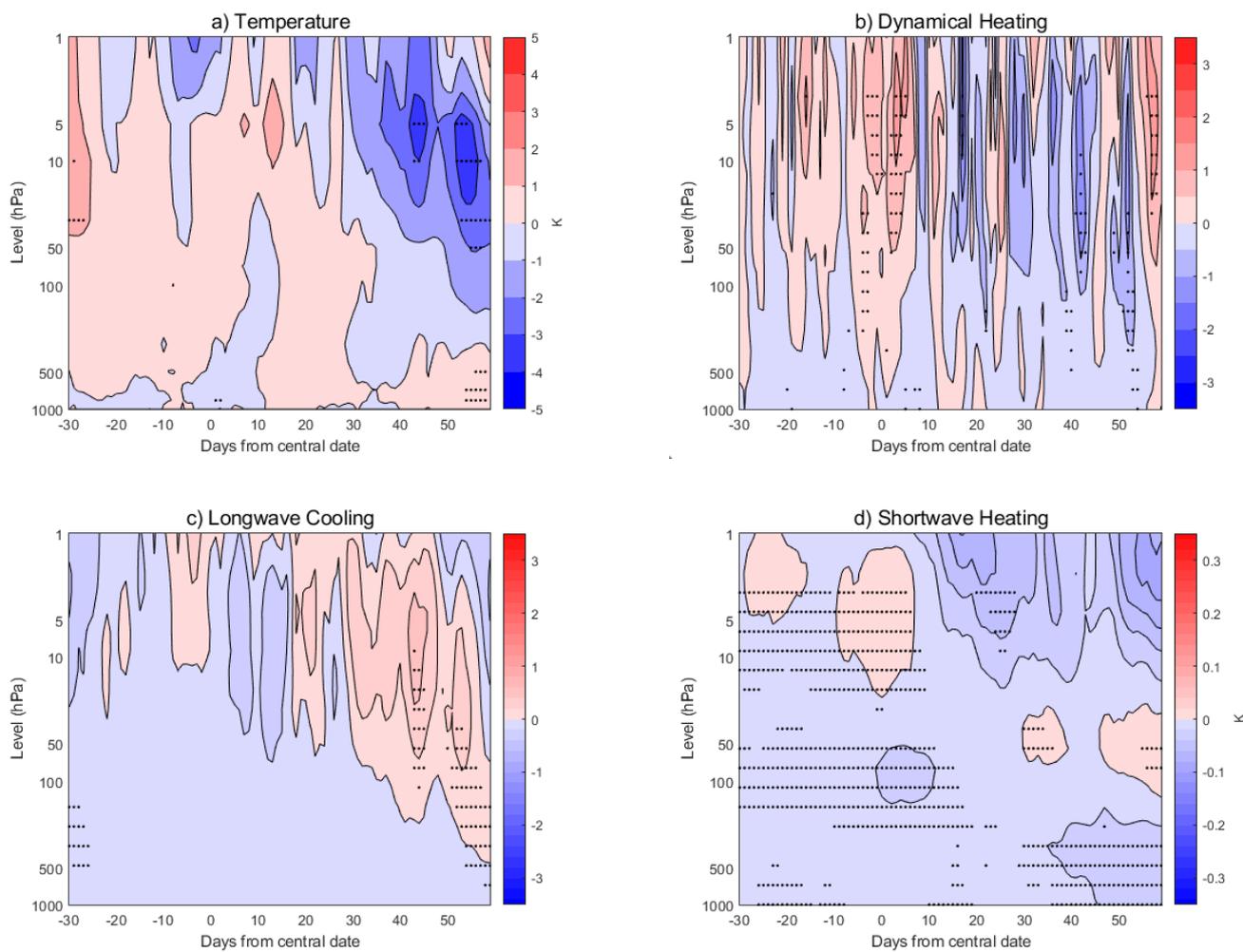
Figure 14. As in Figure 5, for DJF SPVs.
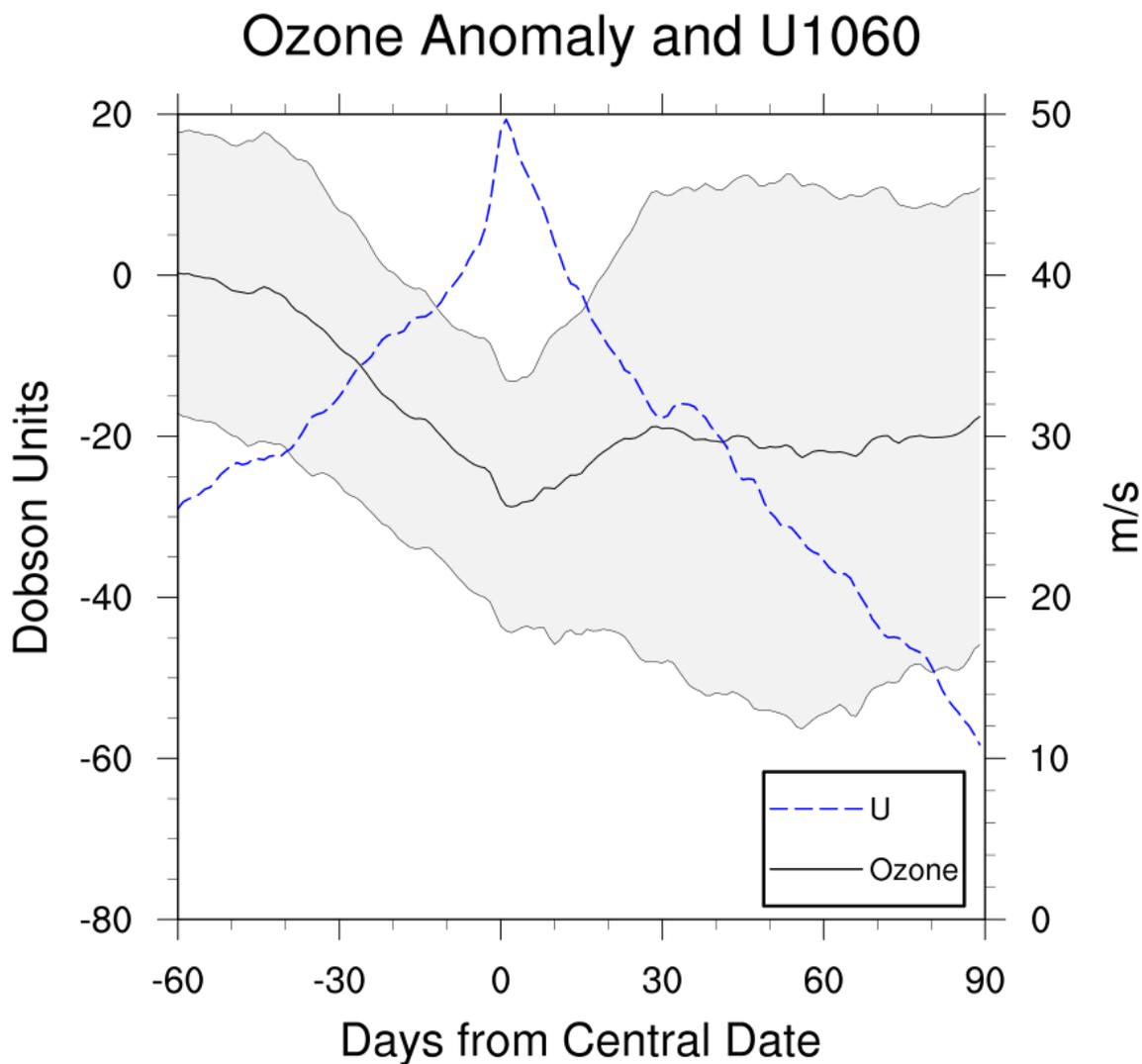
Figure 15. As in Figure 7, for DJF SPVs.